

Two-electron detachment and excitation processes in S^- collisions with atoms and molecules

S. Boumsellek, Vu Ngoc Tuan, and V. A. Esaulov

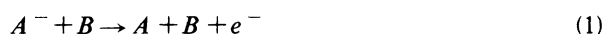
*Laboratoire des Collisions Atomiques et Moléculaires, Bâtiment 351,
Université Paris-Sud, Orsay 91405, France*

(Received 21 March 1989)

Results of an electron-spectroscopy study of two-electron detachment (ionization) and excitation processes in S^- collisions with He, Ne, Ar, Kr, H_2 , O_2 , and N_2 are presented. The electron spectra indicate that singly excited autoionizing states of S ($^2D\ nl$ and $^2P\ nl$ series) are populated in these collisions, and this should lead to substantial S^+ production. Previously unknown autoionizing states of the $^2D(^2P)nl$ series are identified. In the case of the O_2 target, charge exchange to the lowest $O_2^- (^2\Pi_g)$ shape resonance is observed.

I. INTRODUCTION

We present results of a study of excitation and two-electron detachment processes in collisions of S^- with atoms and molecules. In earlier studies we investigated in some detail one-electron detachment in collisions of a variety of negative ions (see, e.g., Esaulov¹) with atomic and molecular targets at low collision energies where a molecular description is valid. The main motivation was the study of ionization processes for systems where this process is accessible directly and not as a result of a prior interaction with the Rydberg series of excited states. The general characteristics of this direct electron-detachment process



now appear clear, though calculations for specific complex systems are still lacking.

Excitation processes in negative-ion collisions have not yet obtained a satisfactory description. There do not exist any *ab initio* calculations of known low-energy excitation cross sections. Attempts have been made² to analyze qualitatively data on excitation within the usual molecular-orbital diagram framework used in atom-atom collisions; however, the applicability of such an approach is doubtful and approaches have been used³ in which the extra negative-ion electron and core collision are treated separately. At present no definitive description is in view. On the experimental side, early work had focused mainly on the electron-spectroscopy study of autodetaching states of negative ions (see, e.g., the review of Edwards⁴). Until recently, the data on neutral excited-state production in collisions of negative ions other than H^- came from energy-loss measurements¹⁻³ that gave general indications about excitation processes, but it is only in the past few years that optical and electron-spectroscopy studies have brought precise information about the excited states produced and some insight into two-electron detachment processes. Thus there are indications³⁻⁵ that ionization (two-electron loss) in low-energy collisions may be due to the population of singly excited autoionizing states. A large number of elements

possess such states. As an example one can consider some common elements with partially filled p shells (groups V, VI, and VII). For these, the ground configuration of the positive ion corresponds to several states, e.g., $^4S^\circ$, $^2D^\circ$, and $^2P^\circ$ for sulfur or 3P , 1D , and 1S for the halogen series. The upper members of the Rydberg series converging to the higher ionization limits [$^2D)nl$ and $^2P)nl$ for sulfur] lie above the first (or second) ionization limits and are therefore autoionizing. In a negative-ion collision the detached electron energy spectrum will contain contributions from single- and double-electron loss. In the case of positive-ion production as a result of formation of autoionizing states, the spectrum will contain corresponding characteristic peaks. The detached-electron energy spectra (DEES) thus shed light on excited-state formation and two-electron detachment. The study of these spectra as a function of collision energy can allow the estimate of the onset of two-electron detachment and its relative importance to one-electron detachment processes. These spectra are clearly also interesting from a purely spectroscopic point of view since they give information that is complementary to optical studies of autoionizing states, where dipole selection rules impose a restriction on the possible excited states.

In this paper we present results of an electron-spectroscopy study of S^- collisions with inert gases and molecules. Earlier studies of one- and two-electron loss in S^- collisions are limited to total cross-section measurements in the 12.5–240-keV energy range⁶ for the inert gases, H_2 , O_2 , and N_2 targets. At a 12.5-keV collision energy the ratio of the 2:1 electron detachment cross sections were found to be of 22.7% (He), 8.5% (Ne), 26.5% (Ar), and 22.2% (Kr). Smaller values are obtained for molecular targets. At low collision energies there only exist total electron detachment cross-section measurements.^{7,8} For the H_2 target there are also measurements for H^- production in reactive processes.⁸

II. EXPERIMENTAL SETUP

The measurements were performed on a newly constructed apparatus for gas-phase and surface studies. A schematic diagram of the layout of the setup, consisting

of three differentially pumped chambers, is shown in Fig. 1.

A simple discharge ion source is used. For S^- ions a carbon oxy-sulfide and argon (OCS)+Ar gas mixture was used in the source. The source and the three cylindrical element ion-extraction optics were readapted from an older system.³ The extracted ions are mass analyzed by a 10-cm-long, rare-earth-cobalt-permanent-magnet Wien filter with a magnetic field of about 800 G within a 22-mm spacing. The Wien filter is enclosed in a cast iron box to reduce magnetic fields along the beam line beyond it.

The ions are deflected through 90° by a quadrupole deflector.⁹ This deflection prevents stray neutrals and photons emitted by the ion source from reaching the collision region. Initially we made some attempts to use the quadrupole deflector without the shim plates present in the original design.⁹ This resulted in a severe (50%) decrease in transmitted beam intensity and attempts to refocus the beam with an extra lens placed at the exit of the deflector proved to be unsuccessful. It is interesting to note that without the shim plates, the best performance was obtained with strongly asymmetric voltages ($V^+ = 2V^-$ or vice versa). After inclusion of shim plates, essentially all of the beam could be collected through a 5-mm-diam aperture placed at 20 cm beyond the quadrupole and refocused by lens L_2 , using the normal symmetric voltage mode.

The deflected ions enter the main chamber which is equipped with a secondary lens stack and a Menzinger-type¹⁰ decelerator, which has allowed us to obtain beams

of energies down to 5 eV. The ions are monitored by a Faraday cage, which allows improved beam focusing, by using a dual ring and plate system.

The main chamber contains a goniometer consisting of two coaxial rings. The inner ring supports the electron spectrometer, whereas the outer one will support an ion spectrometer. A continuous setting from $+135^\circ$ to -135° with a 0.2° (inner ring) and 0.1° (outer ring) resolution may be obtained. A dual μ metal magnetic shielding is employed to reduce magnetic fields resulting in a reduction of the vertical component to about 6 mG and the horizontal component to 1 to 2 mG. A further reduction in the vertical component of the magnetic field to about 1 mG is achieved by using Helmholtz coils.

A 45° parallel plate electrostatic analyzer was employed in the present measurements and is described in detail elsewhere.¹¹ The theoretical resolution for the system is approximately 30 meV for a 2.5-eV pass energy. In order to obtain low-energy electron spectra (below 2 eV) the optics at the entrance of the analyzer was operated in a zoom mode. The scanning was implemented using digital-to-analog converters. The data acquisition and optics control were performed with an Intel 8086 based computer, electronics, and program that are described elsewhere.¹² The voltages for the zoom optics for various electron energies were determined by manual optimization and tabulated in the computer, which then sent out linearly iterated values of the voltages depending upon the analyzed electron energy.

One of the main difficulties, which at present limits these measurements, consists of the determination of the transmission function, i.e., the transmitted electron intensity for a given electron energy. The use of zoom optics, which increases significantly the efficiency of data acquisition, also results in a strong sensitivity of the shape of the acquired spectrum (for low electron energies) to the size of the collision volume and to variations in the position of the beam. In principle, the transmitted electron intensity decreases with electron energy. However, small space charges can drastically modify the spectra for the lowest transmitted electron energies. In earlier studies attempts have been made⁵ to determine the transmission function by first measuring the electron spectrum in ionizing electron-helium collisions, which in virtue of Wannier's threshold law, should be a constant. The correction function obtained from these measurements was then used to renormalize the electron spectra in ion-atom collisions. However, the results thus obtained are still subject to a controversy⁵ and here we shall not discuss at any length the shape of the spectra as a function of electron energy, though in general very similar settings of the optics were used and the transmission function should not be very different for the series of spectra presented here, except at the lowest energies ($E < 200$ meV).

A last point to be noted is that for low electron energies and forward observation angles (small angles between the ion beam and analyzer) a substantial background signal is observed. This is in part due to the incident ions hitting the analyzer. A fairly efficient means of eliminating this is implemented by recording spectra

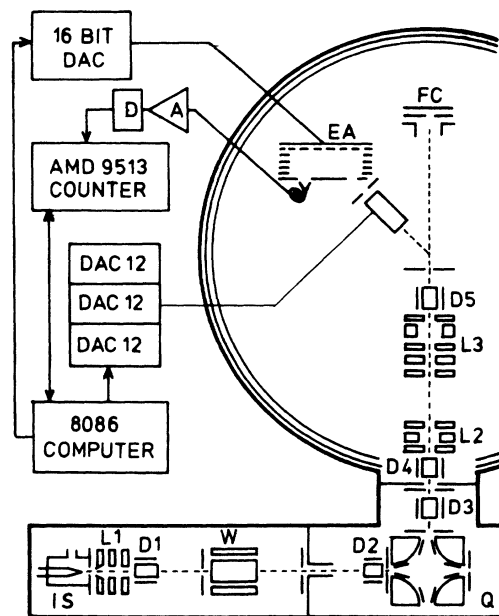


FIG. 1. Schematic diagram of the experimental setup, showing the chamber configuration, ion source (IS), Wien filter (W), quadrupole deflector (Q), various lenses (L_1 - L_3), deflectors (D_1 - D_5), Faraday cage (FC), electrostatic analyzer (EA), and the associated data-handling arrangement.

with the target gas passing through the main capillary and through a secondary, similar, gas inlet placed far from the collision region, but which results in a similar background pressure. The two spectra are collected alternatively, sweep by sweep, and are then subtracted. Most of the results presented here were obtained in this mode.

The energy calibration of the analyzer was initially established by recording energy spectra of electrons emitted in O^- collisions with Ne. These were previously reported by Penent *et al.*,⁵ who gave the energies of peaks due to autoionizing states with an accuracy of 20 meV.

III. RESULTS AND DISCUSSION

A. General characteristics of the electron spectra

The integral spectrum we measure contains contributions from one- and two-electron detachment processes. Some of these, like the direct detachment process (1), lead to continuous electron energy distributions. Excitation of autoionizing states and autodetaching states on the other hand results in well-defined peaks. The attribution of these to the projectile or target atom is based on the Doppler shift of the peaks due to the projectile as a function of observation angle and (or) collision energy. The spectra were therefore recorded for several angles and results for a 25° observation angle are shown in Figs. 2–5 for some of the studied energies.

As may be seen, the electron spectra consist of a continuous distribution, on which is superimposed a series of peaks which we attribute to autoionizing peaks of sulfur. The width of the peaks in the spectrum is determined by several effects: (i) the analyzer resolution; (ii) electron ejection kinematics ($\delta E_k = 16$ meV for a 0.63-eV electron, a 2-keV collision energy, a $\theta = 25^\circ$ observation angle, and $d\theta = 5^\circ$); and (iii) "natural" broadening effects that may

TABLE I. Autoionizing states of S observed in S^- collisions (see Fig. 5 for peak labels).

Peak	$E_{c.m.}$ (eV)	n^*	States Initial	Final S^+
A	0.028	2.73	$3d' ^3D^\circ$	$4S^\circ$
B	0.157			
C	0.236	2.89	$3d' ^3F^\circ$ $5s' ^3D^\circ$	$4S^\circ$ $4S^\circ$
D	0.289	2.93	$3d' ^3S^\circ$	$4S^\circ$
E	0.335	3.03	$3d' ^3P^\circ$	$4S^\circ$
F	0.493	3.17	$3d' ^3G$	$4S^\circ$
		2.31	$4p''$	$4S^\circ$
		4.38	$6p''$	$2D^\circ$
G	0.632	3.35	$5p' ^3F$	$4S^\circ$
H	0.698	3.45	$5p' ^3P$	$4S^\circ$
I	0.782	3.59	$4d' ^1P^\circ$	$4S^\circ$
		5.69	$7p''$	$2D^\circ$
J	0.952	3.91	$4d' ^3P^\circ$ $6s' ^3D^\circ$ $4d' ^3S^\circ$	$4S^\circ$ $4S^\circ$ $4S^\circ$
K	1.115	4.32	$6p' ^3F, ^3P$	$4S^\circ$
L	1.262	2.75/4.83	$3d'' / 5d'$	$4S^\circ$
M	1.341	5.2	$7p' ^3F$	$4S^\circ$

occur, in particular, due to some quasimolecular decay during the collision.

The position of the peaks in Figs. 2–5 is different for different collision energies because of kinematics effects. The energies at which these peaks appear in the center-of-mass frame are given in Table I along with the pro-

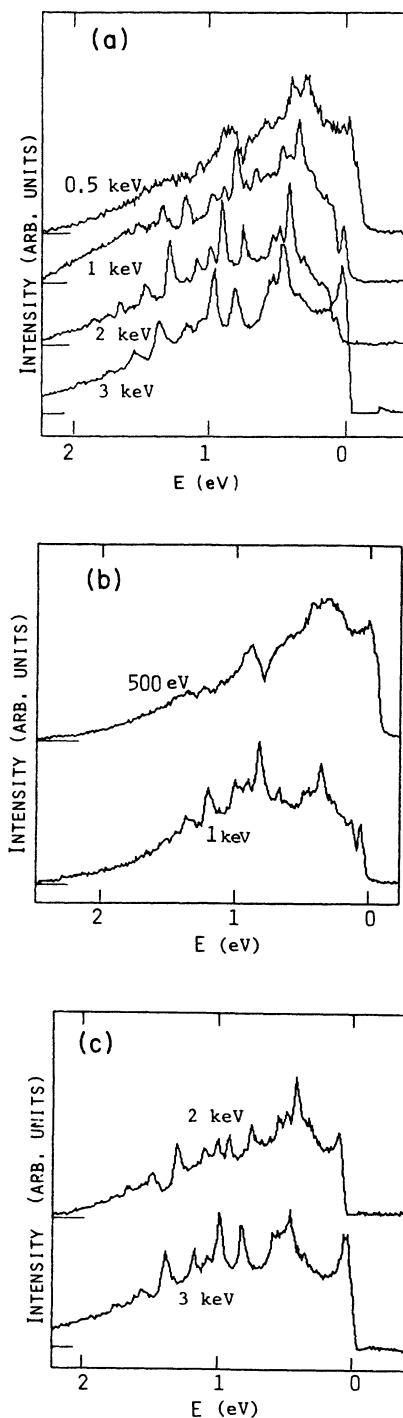


FIG. 2. Energy spectra of electrons ejected in S^- collisions with (a) Ar and (b) and (c) Kr for the indicated collision energies.

posed assignments. The peaks at the lowest energies pose some problems. Here, the transmission function is generally the largest and there also exists a large number of stray scattered low-energy electrons. These effects result in the appearance of an intense zero-energy peak. This peak is strongly reduced in the present spectra because of the subtraction procedure we employ. However, the identification of peaks in this lowest-energy region is rendered difficult. Nevertheless, in some cases, as in the 2-keV Ar spectrum, the large "noise" peak at zero energy was not observed (presumably because of a change in the transmission function) and therefore the observed structure (peak A) was included in Table I and has a realistic assignment.

For some of the considered targets, the continuous electron distribution, which is presumably mainly due to reaction (1), presents no significant features. However, for instance, for the Ne target the spectrum clearly appears to be composed of different distributions. The origin of this may be sought in the characteristics of the S^- plus inert-gas system, which is similar to the O^- inert-gas one discussed in detail by Esaulov *et al.*^{1,13} Here we recall briefly that there exist two entrance (or initial) molecular states in these collisions. These are the $^2\Sigma(\pi^4\sigma)$ and

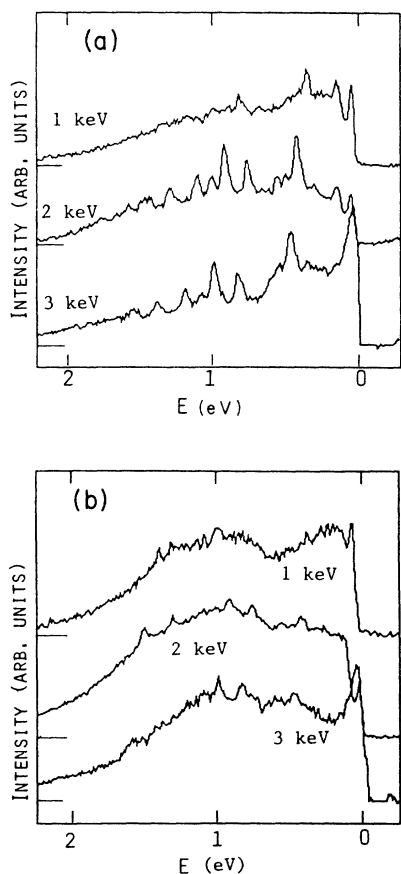


FIG. 3. Energy spectra of electrons ejected in S^- collisions with (a) He and (b) Ne.

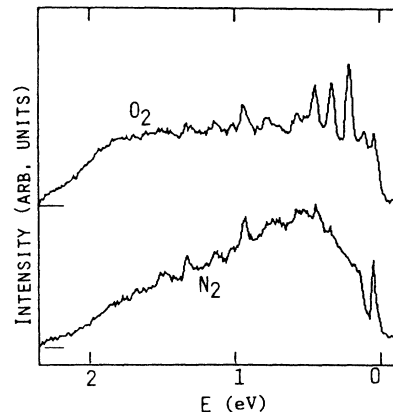


FIG. 4. Energy spectra of electrons ejected in 2-keV collisions of S^- with (a) N_2 and (b) O_2 .

$^2\Pi(\pi^3\sigma^2)$ states that correlate to $S^- (^2P)$ plus inert gas (1S) at infinity. Also there exist a number of exit channels corresponding to $S (^3P, ^1D, \text{ and } ^1S)$ plus inert gas at infinity. These are (i) the $^3\Pi(\pi^3\sigma)$ and $^3\Sigma(\pi^2\sigma^2)$ states dissociating to $S (^3P)$ plus inert gas, (ii) the $^1\Sigma^+(\pi^4)$, $^1\Pi(\pi^3\sigma)$, and $^1\Delta(\pi^2\sigma^2)$ states dissociating to $S (^1D)$ plus inert gas, and (iii) the $^1\Sigma^+(\pi^4)$ state dissociating to $S (^1S)$ plus inert gas.

Assuming^{1,13} the detachment of an outer σ electron we see that scattering in the $^2\Sigma(\pi^4\sigma)$ state leads to the population of the $^1\Sigma^+(\pi^4)$ state, whereas scattering in the $^2\Pi(\pi^3\sigma^2)$ states will lead to the population of the $^3\Pi(\pi^3\sigma)$ [and eventually the $^1\Pi(\pi^3\sigma)$] states. Also quasi-molecular Auger detachment may occur from the $^2\Pi(\pi^3\sigma^2)$ states leading to population of the $^1\Sigma(\pi^4)$ states. For the low collision velocities that we consider, one may expect that direct detachment (1) will lead to the population of the lowest 3P and 1D states, as in the case of O^- . We thus see that there exist several channels for detachment which can all lead to different electron energy distributions (as was indeed also noted¹² for O^-). This then may be the cause of the structured spectrum in the $S^- - \text{Ne}$ case.

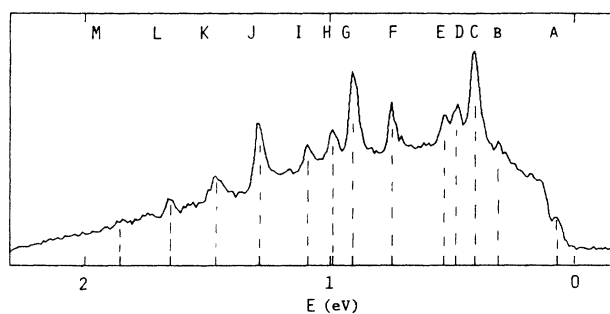


FIG. 5. Energy spectrum of electrons ejected in a 2-keV collision of S^- with Ar. The peaks are labeled with reference to Table I.

Turning now to the question of peaks due to autoionizing states we first note that these are found to increase in intensity with increasing collision energy and are more intense for forward scattering angles. The latter feature is due to the following several effects: (i) electron ejection kinematics, (ii) symmetry of the states involved, and (iii) additional anisotropic effects such as the ones observed previously in H^- collisions,¹⁴ but for which there does not yet exist any explanation. A more detailed angular dependence study will have to await the knowledge of the transmission function for different angles.

For the Ar and Kr targets these peaks appear at energies below 500 eV (Fig. 2). At this energy mainly the lowest states are observed. With increasing energy higher-lying states are populated. Though we do not know exactly the transmission function, an estimate of the relative magnitude of the processes responsible for these peaks and for the broad electron distributions as a function of collision energy may be made by integrating the area under the peaks and the rest of the spectrum for which we assume a smooth, continuous form. This procedure yields the following figures: 10%, 17%, 22%, and 24% for 500 eV, 1000 eV, 2 keV, and 3 keV, respectively, for Ar; and 22% for collisions with Kr at 3 keV.

In the case of the He and Ne targets (Fig. 3) the onset energies for the autoionizing state production lie in the 1 keV laboratory collision energy range (this corresponds to 111 eV in the center-of-mass frame for $S^- + He$). The corresponding cross section appears to grow very rapidly with increasing collision energy, though in the Ne case excitation of these peaks remains small even at the highest studied 3-keV energy. An interesting feature of the $S^- + He$ spectrum is that it is not marked by any particular selectivity in the excitation process. Indeed, peaks due to quite high-lying states are present in the spectrum. This would suggest the opening up of a single common excitation channel. As for the Ar and Kr targets, we performed an integration of the areas under the peaks and the broad distribution yielding a ratio of 22% for 3-keV collisions with He. For Ne this ratio is less than 6% at this energy.

In the case of the molecular O_2 and N_2 targets the electron spectrum (Fig. 5) also contains a minor contribution from these autoionizing states. In the H_2 case these were not observed. Note that for O_2 the spectrum also displays peaks due to charge exchange to the O_2 (${}^2\Pi_g$) shape resonance.¹ Decay of this resonance $O_2^-(v \geq 0) \rightarrow O_2(v' \geq 0)$ is at the origin of the sharp low-energy peaks with a spacing of 0.12 eV characteristic of O_2^- .

It is interesting to compare the ratios of the known total cross sections⁶ for one- and two-electron loss cited in the Introduction with the ones obtained above. As may be observed, the magnitude of the 3-keV data is consistent with the, somewhat higher energy, total cross-section data. Also, the fact that the two-electron total detachment cross section is smaller in the case of Ne and the molecular targets is consistent with our finding of a smaller cross section of autoionizing-state production. This comparison should of course be treated with caution since the ratios may be affected by the transmission func-

tion, but it does indicate that *excitation of autoionizing states contributes significantly to ionization.*

B. The autoionizing states

The ground-state configuration of S^+ corresponds to the three ${}^4S^o$, ${}^2D^o$, and ${}^2P^o$ states which are separated by 1.84 eV (${}^4S^o - {}^2D^o$) and 1.2 eV (${}^2D^o - {}^2P^o$). There thus exist three families of singly excited states. Only the lowest ${}^2D^o$ ($4s$, $4p$, and singlet $3d$) and ${}^2P^o$ ($4s$) states lie below the first ${}^4S^o$ ionization limit. Other states lie in the continuum region and some may autoionize. Autoionizing states of sulfur have been studied experimentally^{15,14,17} and theoretically¹⁶ in several recent photoionization studies. These authors report triplet states of the ns and nd series. Singlet $3d' {}^1P^o$, $3d' {}^1F^o$, $5s' {}^1D^o$, and $5s'' {}^1P^o$ states have been reported by Kaufmann.¹⁷ States of the ${}^2D np$ and ${}^2P np$ series were not known till now. A discussion of various aspects of autoionizing states of S may be found in these papers and will not be reproduced here. It should only be pointed out that in case of sulfur (and oxygen) deviations from LS coupling are observed and one is led to consider less stringent rules, which follow from the inclusion of other interactions. Autoionizing transitions must obey angular momentum and parity conservation. Describing the continuum state in the same way as the discrete state by specifying the spin and angular momentum quantum numbers for the state of the ion and free electron, the selection rules for LS coupling are $\Delta L = 0$, $\Delta S = 0$. Upon inclusion of effects of spin-orbit interaction one has¹⁸ $\Delta L = 0, \pm 1$ and $\Delta S = 0, \pm 1$, while inclusion of spin-spin interaction leads to $\Delta L = 0, \pm 1, \pm 2$ and $\Delta S = 0, \pm 1, \pm 2$. The inclusion of the effects of other interactions thus greatly increases the number of possible autoionizing transitions. Note also that mixing with other states may render some transition possible.

In order to assign the peaks in our spectra (Fig. 5) we first referred directly to earlier studies. This allowed the assignment of some of the peaks, though for the high-lying ones some ambiguities exist due to lack of resolution. There also exists an ambiguity concerning the assignment of peak C. According to the data of Gibson *et al.*¹⁵ this could be the $5s' {}^3D^o$ state whereas according to the data of Joshi *et al.*¹⁵ this could be the $3d' {}^3F^o$ state which is forbidden to autoionize in the LS coupling scheme.

The peaks B, F-I, K, and M could not be identified in this manner. Starting from the usual expression for the energies (E) of states

$$E = V_{\text{ion}} - \frac{R}{(n - \delta)^2},$$

where V_{ion} is the ionization potential, R the Rydberg constant, and n the principal quantum number, we computed values of the effective quantum number $n^* = n - \delta$, associated with these transitions. We assumed parentage to both the ${}^2D nl$ and ${}^2P nl$ series and allowed for decay into the ${}^4S^o$ and ${}^2D^o$ continua. We also calculated n^* for the known¹⁸ np' states which are found to be 2.33, 2.34, 2.36, and 2.4 for the $4p' {}^3D$, 3F , 1F , and 3P states, respectively. As reported in earlier studies¹³⁻¹⁶ the quantum defects for the ns' series are approximately 2.1. For the

nd' series these lie in the -0.46 – 0.3 range and are -0.46 and -0.36 for the specific case of $3d' {}^1P^\circ$ state and $3d' {}^1F^\circ$ states, respectively.¹⁷ A comparison of these values suggests the assignments of the $5p'$, $6p'$, and $7p'$ states given in Table I. A possible assignment of peak F could be the previously unknown $3d' {}^{1,3}G$ states with a quantum defect of 0.17. Peak I could be due to the $4d' {}^1P^\circ$. Alternatively, the peaks F and I could be due to the ${}^2P np$ series assuming that, as for oxygen,^{19,20} the quantum defect should be similar. At present peak B remains unassigned.

IV. CONCLUDING REMARKS

The results here show that at low energies excitation of autoionizing states is important in S^- collisions with atoms and molecules and that this channel contributes significantly to S^+ production. This result is in agreement with earlier measurements for O^- and halogen anion collisions. Thus it is clear that a significant part of the primary excitation mechanism is channeled into ionization. It would be most interesting to compare results for S^- collisions with those for S collisions. This would be helpful in particular in unveiling the eventual existence of ionization channels, which result in a continuous electron energy distribution and which, in the case of

the negative ion, would be masked by the one-electron detachment process. To achieve this a small modification of the apparatus is now being performed to allow for production of a neutral S beam. An analysis of the excitation and ionization processes within a quasimolecular framework will be presented subsequently when the data on the neutral system is available.

ACKNOWLEDGEMENTS

This work was supported in part by the Direction des Recherches Etudes et Techniques, France, under Contract No. 84/154. We are greatly indebted to the University of Kaiserslautern and Dr. F. Linder for invaluable assistance in the construction of the goniometer. We would also like to thank Dr. J. R. Peterson and D. H. Helm of the Stanford Research Institute for providing data on the design of the quadrupole deflector. Special thanks are due to A. Abadia, G. Le Bourhis, J. P. Guillotin, R. Paineau, D. Ragonnet, and P. Rudnyckij, for their expert technical assistance in the construction and setting up of the apparatus. The Laboratoire des Collisions Atomiques et Moleculaires is "Unité de Recherche Associé au Centre Nationale de la Recherche Scientifique No. 281."

¹V. A. Esaulov, *Ann. Phys. (Paris)* **11**, 493 (1986).

²J. Fayeton, D. Dhucq, and M. Barat, *J. Phys. B* **11**, 1267 (1978).

³V. A. Esaulov, D. Dhucq, and J. P. Gauyacq, *J. Phys. B* **11**, 1049 (1978); J. P. Grouard, V. A. Esaulov, R. I. Hall, J. L. Montmagnon, and Vu Ngoc Tuan, *ibid.* **19**, 1483 (1986).

⁴A. K. Edwards, *Invited Lectures, Review Papers and Progress Reports of the Ninth International Conference on the Physics of Electronic and Atomic Collisions, Seattle, 1975*, edited by J. Risley and R. Geballe (University of Washington Press, Seattle, 1975), pp. 790–802.

⁵F. Penet, J. P. Grouard, R. I. Hall, J. L. Montmagnon, R. L. Champion, L. D. Doverspike, and V. A. Esaulov, *J. Phys. B* **20**, 6065 (1987).

⁶B. Hird, M. Bruyere, and S. Fafard, *Can. J. Phys.* **65**, 735 (1987); W. J. Lichtenberg, K. Bethge, and H. Schmidt-Bocking, *J. Phys. B* **13**, 343 (1980).

⁷J. B. Hasted, *Proc. R. Soc. London, Ser. A* **212**, 235 (1952).

⁸M. S. Huq, D. Scott, L. D. Doverspike, and R. L. Champion, *J. Chem. Phys.* **82**, 3118 (1985).

⁹H. D. Zeman, *Rev. Sci. Instrum.* **48**, 1079 (1977).

¹⁰Colutron Research, Boulder, CO.

¹¹S. Boumsellek, Vu Ngoc Tuan, and V. A. Esaulov, in *Proceedings of the 16th International Conference on the Physics of Electronic and Atomic Collisions*, edited by A. Dalgarno, R. S. Freund, M. S. Lubell, and T. B. Lucatorto (Plenum, New York, 1989); and (unpublished).

¹²V. A. Esaulov and R. Bartolo, *Microbull. CNRS* **21**, 50 (1986).

¹³V. A. Esaulov, J. P. Gauyacq, and L. D. Doverspike, *J. Phys. B* **13**, 193 (1980).

¹⁴V. A. Esaulov, J. P. Grouard, R. I. Hall, and J. L. Montmagnon, *Phys. Rev. A* **35**, 2470 (1987).

¹⁵S. T. Gibson, J. P. Greene, B. Ruscic, and J. Berkowitz, *J. Phys. B* **19**, 2825 (1986); Y. N. Joshi, M. Mazzoni, A. Nencioni, W. H. Parkinson, and A. Cantu, *ibid.* **20**, 1203 (1987).

¹⁶C. Mendoza and C. Zeippen, *J. Phys. B* **21**, 259 (1986).

¹⁷V. Kaufman, *Phys. Scr.* **26**, 439 (1982).

¹⁸P. Feldman and R. Novick, *Phys. Rev.* **160**, 143 (1967).

¹⁹C. Moore, *Atomic Energy Levels*, Natl. Bur. Stand. (U.S.) Circ. No. 467 (U.S. GPO, Washington, D.C., 1949).

²⁰M. E. Rudd and K. Smith, *Phys. Rev.* **169**, 79 (1968).